



This article is published as part of a themed issue of ***Photochemical & Photobiological Sciences*** on

[Drug delivery technologies and immunological aspects of photodynamic therapy](#)

Guest edited by **Kristian Berg, Jakub Golab, Mladen Korbelik and David Russell**

Published in **[issue 5, 2011](#)**

Perspectives

[Photodynamic therapy enhancement of anti-tumor immunity](#)

C. M. Brackett and S. O. Gollnick, *Photochem. Photobiol. Sci.*, 2011, **10**, 649

[PDT-induced inflammatory and host responses](#)

M. Firczuk, D. Nowis and J. Gołab, *Photochem. Photobiol. Sci.*, 2011, **10**, 653

[Cancer vaccines generated by photodynamic therapy](#)

M. Korbelik, *Photochem. Photobiol. Sci.*, 2011, **10**, 664

[DAMPs and PDT-mediated photo-oxidative stress: exploring the unknown](#)

A. D. Garg, D. V. Krysko, P. Vandenabeele and P. Agostinis, *Photochem. Photobiol. Sci.*, 2011, **10**, 670

[Antitumor immunity promoted by vascular occluding therapy: lessons from vascular-targeted photodynamic therapy \(VTP\)](#)

D. Preise, A. Scherz and Y. Salomon, *Photochem. Photobiol. Sci.*, 2011, **10**, 681

[On the cutting edge: protease-sensitive prodrugs for the delivery of photoactive compounds](#)

D. Gabriel, M. F. Zuluaga and N. Lange, *Photochem. Photobiol. Sci.*, 2011, **10**, 689

[Combination of photodynamic therapy and immunomodulation for skin diseases—update of clinical aspects](#)

X.-L. Wang, H.-W. Wang, K.-H. Yuan, F.-L. Li and Z. Huang, *Photochem. Photobiol. Sci.*, 2011, **10**, 704

[Nanoparticles: their potential use in antibacterial photodynamic therapy](#)

S. Perni, P. Prokopovich, J. Pratten, I. P. Parkin and M. Wilson, *Photochem. Photobiol. Sci.*, 2011, **10**, 712

[Photosensitizer–antibody conjugates for photodynamic therapy](#)

A. J. Bullous, C. M. A. Alonso and R. W. Boyle, *Photochem. Photobiol. Sci.*, 2011, **10**, 721

[The immunosuppressive side of PDT](#)

P. Mroz and M. R. Hamblin, *Photochem. Photobiol. Sci.*, 2011, **10**, 751

[Synthetic approaches for the conjugation of porphyrins and related macrocycles to peptides and proteins](#)

F. Giuntini, C. M. A. Alonso and R. W. Boyle, *Photochem. Photobiol. Sci.*, 2011, **10**, 792

[Combination approaches to potentiate immune response after photodynamic therapy for cancer](#)

T. G. St. Denis, K. Aziz, A. A. Waheed, Y.-Y. Huang, S. K. Sharma, P. Mroz and M. R. Hamblin, *Photochem. Photobiol. Sci.*, 2011, **10**, 802

[Clinical and immunological response to photodynamic therapy in the treatment of vulval intraepithelial neoplasia](#)

S. Daayana, U. Winters, P. L. Stern and H. C. Kitchener, *Photochem. Photobiol. Sci.*, 2011, **10**, 810

Papers

[Cytosolic delivery of LDL nanoparticle cargo using photochemical internalization](#)

H. Jin, J. F. Lovell, J. Chen, K. Ng, W. Cao, L. Ding, Z. Zhang and G. Zheng, *Photochem. Photobiol. Sci.*, 2011, **10**, 817

[Preliminary safety and efficacy results of laser immunotherapy for the treatment of metastatic breast cancer patients](#)

X. Li, G. L. Ferrel, M. C. Guerra, T. Hode, J. A. Lunn, O. Adalsteinsson, R. E. Nordquist, H. Liu and W. R. Chen, *Photochem. Photobiol. Sci.*, 2011, **10**, 822

[Targeted photodynamic therapy of breast cancer cells using antibody–phthalocyanine–gold nanoparticle conjugates](#)

T. Stuchinskaya, M. Moreno, M. J. Cook, D. R. Edwards and D. A. Russell, *Photochem. Photobiol. Sci.*, 2011, **10**, 832

[Methylene blue covalently loaded polyacrylamide nanoparticles for enhanced tumor-targeted photodynamic therapy](#)

M. Qin, H. J. Hah, G. Kim, G. Nie, Y.-E. Koo Lee and R. Kopelman, *Photochem. Photobiol. Sci.*, 2011, **10**, 842

[Quantum dot–folic acid conjugates as potential photosensitizers in photodynamic therapy of cancer](#)

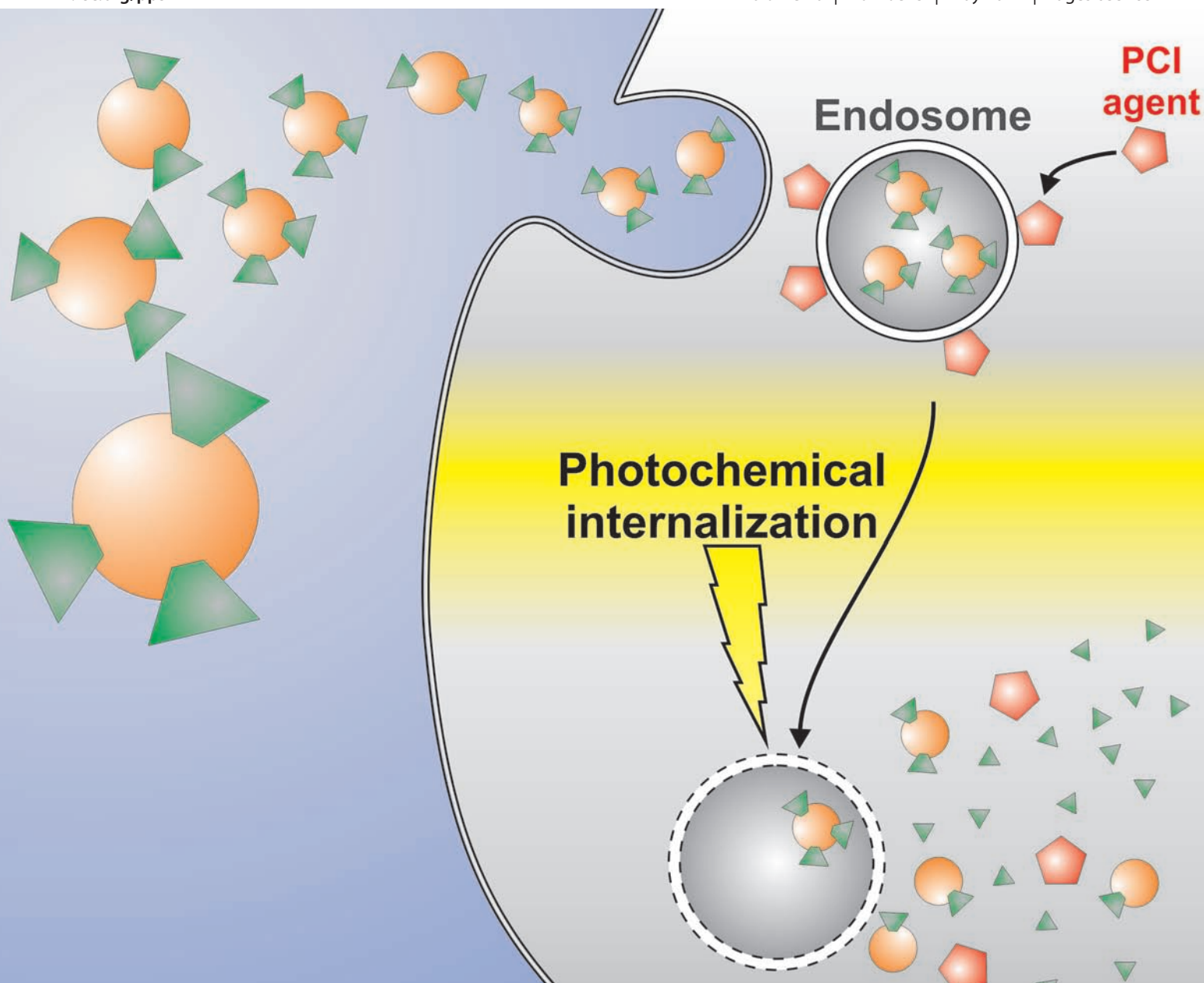
V. Morosini, T. Bastogne, C. Frochot, R. Schneider, A. François, F. Guillemain and M. Barberi-Heyob, *Photochem. Photobiol. Sci.*, 2011, **10**, 852

Photochemical & Photobiological Sciences

An international journal

www.rsc.org/pps

Volume 10 | Number 5 | May 2011 | Pages 635–854



Themed issue: Drug delivery and immunological aspects of photodynamic therapy

ISSN 1474-905X

RSC Publishing



1474-905X(2011)10:5;1-3

Cytosolic delivery of LDL nanoparticle cargo using photochemical internalization†

Honglin Jin,^{a,b,d} Jonathan F. Lovell,^{a,c} Juan Chen,^a Kenneth Ng,^{a,c} Weiguo Cao,^a Lili Ding,^a Zhihong Zhang^{a,d} and Gang Zheng^{*a,b,c}

Received 17th November 2010, Accepted 1st February 2011

DOI: 10.1039/c0pp00350f

Following cellular delivery, most drugs must escape endosomes and lysosomes and reach the cytosol to be effective. This is particularly significant for nanoparticles, which can carry a large drug payload, but typically accumulate in endosomes and lysosomes. One attractive solution is to use light-triggered release, which can provide efficient endolysosomal membrane disruption and spatiotemporal control of cytosolic release. Here, we demonstrate the cytosolic release of cargo loaded into low density lipoprotein (LDL) nanoparticles using a photochemical internalization (PCI) approach. Three types of cargo-loaded LDL nanoparticles (CLLNPs) were generated by loading fluorescent dyes *via* (1) intercalation in the phospholipid monolayer exterior (surface loading), (2) conjugation to the amino acids of apoB-100 protein (protein loading) or (3) reconstitution into the hydrophobic core of LDL (core loading). Fluorescence imaging demonstrated the cellular uptake of CLLNPs was mediated by the LDL receptor and resulted in CLLNPs accumulation in endosomes. When cells were co-incubated with CLLNPs and AlPcS2a (a PCI agent), laser irradiation induced efficient cytosolic release of the surface-loaded and protein-labeled cargo, whereas the core-loaded hydrophobic dye could not readily be released. Thus, PCI is a useful cytosolic release method for CLLNPs, although the loading method must be considered.

Introduction

Purified LDL is a viable nanocarrier for targeted delivery of therapeutic drugs since it has homogenous size (18–25 nm) below 40 nm, long circulation time in blood, excellent biocompatibility and customizable targeting capability.^{1–5} There are at least three approaches for incorporating therapeutic agents into LDL: (1) intercalation into the phospholipid monolayer (surface loading); (2) covalent attachment to specific amino acid residues of the apoB-100 protein (protein loading); and (3) reconstitution into the lipid core of LDL (core loading).^{6,7} Cellular uptake of LDL nanoparticles is mediated by the LDL receptor, which is highly expressed in a variety of cancer cells.^{8,9} However, this pathway leads to the entrapment of LDL in lysosomes, where it is hydrolyzed in the presence of a number of enzymes that are active at low pH

(~4.5).¹⁰ Such a trafficking system is not efficient for delivery of therapeutics, which usually exert action on targets located in the cytoplasm.^{11,12} Thus, a strategy permitting endolysosomal escape would provide a valuable step forward for LDL nanoparticle based drug delivery systems.

Photochemical internalization (PCI) is a technique which uses light to facilitate the release of endocytosed macromolecules into the cytoplasm.^{13,14} The mechanism involves breakdown of endosomal/lysosomal membranes by using amphiphilic photosensitizers, such as disulfonated aluminium phthalocyanine (AlPcS2a) and *meso*-tetraphenylporphine disulfonate (TPPS2a), which localize on endosomal/lysosomal membranes.^{13,15} The membranes of these organelles are then destroyed by singlet oxygen generated from photoactivation of the photosensitizers at a sub-lethal dose, resulting in the subsequent release of entrapped drugs into the cytosol. PCI has demonstrated a broad range of biological applications, including releasing endocytosed proteins, peptides, chemotherapeutics, oligonucleotides and small interference RNAs (siRNAs),^{16–20} and was recently approved in a clinic trial in the treatment of solid tumors.²¹ Although PCI was initially developed for release of single molecule drugs, several studies have demonstrated its application in nanomedicine, including for such nanoparticles as dendrimers loaded with doxorubicin,²² liposome loaded with toxin,²³ and nanogels loaded with siRNAs.²⁴ Therefore, PCI possesses great potential for a number of nanocarriers

^aOntario Cancer Institute and Campbell Family Cancer Research Institute, TMDT 5-363, 101 College Street, Toronto, ON, M5G 1L7, Canada. E-mail: gang.zheng@uhnres.utoronto.ca

^bDepartment of Medical Biophysics, University of Toronto, Toronto, Canada

^cInstitute of Biomaterials and Biomedical Engineering, University of Toronto, Toronto, Canada

^dBritton Chance Center for Biomedical Photonics, Wuhan National Laboratory for Optoelectronics-Huazhong University of Science and Technology, Wuhan, China

† This article is published as part of a themed issue on immunological aspects and drug delivery technologies in PDT.

in drug delivery. Here, we investigate PCI for cargo-loaded LDL nanoparticles (CLLNPs) (Fig. 1). This provides an approach for cytosolic release for CLLNPs and a new application of PCI in nanomedicine.

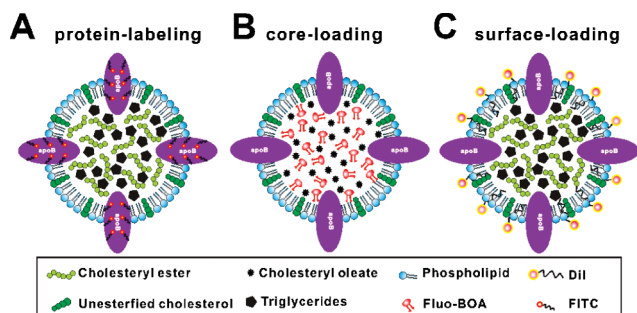


Fig. 1 Schematic representation of CLLNPs. (a) FITC was conjugated to LDL nanoparticles by protein-loading without changing the endogenous components of the core cholesteryl ester and triglycerides. (b) Fluo-BOA dye was incorporated into LDL with a core-loading method. Exogenous cholesteryl oleate was added to improve the protein recovery. (c) DiI dye was surface-loaded onto LDL.

Experimental

Materials

LDL was isolated by sequential ultracentrifugation of human plasma using the established differential centrifugation methods.²⁵ In brief, human plasma was dialyzed in a 0.9% NaCl, 2 mM EDTA solution with 1.006 g mL⁻¹ density, chilled to 4 °C, placed in centrifuge tubes, layered with a buffer of the same composition at room temperature then subjected to ultracentrifugation for 18 h at 40 000 rpm. The top layer containing chylomicrons and VLDL was then removed. LDL was then obtained by repeating the layering and centrifugation steps with a KBr adjusted density of 1.066 g mL⁻¹ in both plasma and layer buffer, centrifuging and collecting the top LDL layer. LDL was further purified using an Akta fast protein liquid chromatography (FPLC) system (Amersham Biosciences) equipped with a HiLoad 16/70 Superose 6 column. Human plasma was obtained from the local blood transfusion services and usage was approved by University Health Network's research ethics board. DiI (D282), Fluorescein (Fluorescein isothiocyanate isomer I-F7250) and AIPcS2a were purchased from Molecular Probes, Sigma and Frontier Scientific, respectively. The Fluo-BOA dye was synthesized as previously described.²⁶

Preparation of CLLNPs

The CLLNPs were prepared by three different methods (Fig. 1). The protein-labelling LDL (LDL-FITC) was prepared by conjugating fluorescein on the lysine residues of apoB protein. Briefly, 2 mg of LDL solution was subjected to buffer exchange twice using the NaHCO₃/Na₂CO₃ buffer (0.08 M NaHCO₃, 0.02 M Na₂CO₃) to adjust pH to 9.4 and final volume to 1 mL using a 100 000 MW cutoff Amicon centrifugal filter device (Millipore, Billerica, MA). Next, 30 µL fluorescein isothiocyanate in DMSO (2 mg mL⁻¹) was slowly added to the LDL solution. After incubating this mixture for 8 h at 4 °C, the resulting LDL-FITC was dialyzed against phosphate buffered saline (PBS)

(pH 7.5 and 0.1 M NaCl) at 4 °C for 2 days to remove the unreacted fluorescein. The protein concentration of LDL-FITC was quantified using a Lowry protein assay with an absorption wavelength of 700 nm and the fluorescein concentration was measured using a UV absorbance-concentration standard curve at 490 nm in methanol. The surface-loading LDL (DiI-LDL) was prepared using a previous described method.²⁷ Briefly, 150 µL of DiI in DMSO (3 mg mL⁻¹) was slowly added to the 1 mL of LDL in PBS solution (1 mg mL⁻¹). After 18 h incubation in dark at 37 °C, the DiI-LDL was isolated by ultracentrifugation for 6 h at 4 °C at 50 000 rpm. This product was further dialyzed against PBS and filtered through 0.2 µm filter, and stored at 4 °C. The protein concentration of DiI-LDL was quantified using a Lowry protein assay at a UV absorption of 500 nm and DiI concentration was measured using an absorbance-concentration standard curve at 554 nm in methanol. Core-loading LDL, (Fluo-BOA)LDL, was prepared using a previously reported procedure.⁴ Briefly, 1.9 mg purified LDL was lyophilized with 25 mg starch in a siliconized glass tube, and then extracted three times with 5 mL of heptane at -5 °C. Following aspiration of the last heptane extraction, 1 mg Fluo-BOA and 4 mg cholesteryl oleate dissolved in 300 µL of toluene were added in the tube. After 20 min incubation at -20 °C, toluene and any residual heptane were removed under a stream of nitrogen gas in an ice salt bath for about 60 min. The (Fluo-BOA)LDL was solubilized in 2 mL Tricine buffer (10 mM, pH 8.4) at 4 °C for 18 h. Starch was removed from the solution by a low-speed centrifugation at 2000 rpm. Next, the solution was transferred to Eppendorf tubes and centrifuged twice at 12 000 rpm for 10 min and further filtered through 0.2 µm filter. The resultant reconstituted LDL was stored at 4 °C. The protein concentration of (Fluo-BOA)LDL was quantified using a Lowry protein assay at an absorption wavelength of 700 nm. The Fluo-BOA concentration was measured by using a UV absorbance-concentration standard curve at 458 nm in methanol. All the CLLNPs were filtered through a 0.2 µm filter (Millipore) before the measurement. The amount of dye contained in each LDL was calculated by dividing the loaded dye concentration by the LDL concentration.

Morphology, size and gel electrophoresis

Transmission electron microscopy (TEM) was performed using a Hitachi H-7000 transmission electron microscope (Hitachi, Inc., Japan) equipped with a digital image acquisition system to determine the morphology of an aqueous dispersion of CLLNPs negative stained with 0.5% uranyl acetate. LDL nanoparticles and CLLNPs were assayed for electrophoretic mobility on a 0.8% agarose gel and the protein content of LDL was stained by Coomassie blue. The thermostability of CLLNPs was performed with light-scattering photon correlation spectroscopy (Zetasizer Nano-ZS90; Malvern Instruments, Malvern, UK) at the temperature of 25, 30, 35, 40, 45, 50, 55 and 60 °C with a pre-incubation of 2 min under each temperature before the measurement.

Confocal imaging of cellular uptake of CLLNPs

Overall experimental flow is shown in Fig. 2. A549 Cells were seeded into 8-well glass-bottom chambers (Nunc Lab-Tek, Sigma-Aldrich) (3 × 10⁴ per well) in RPMI-1640 media (containing

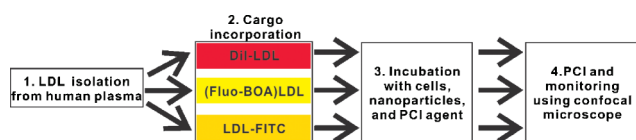


Fig. 2 Flow diagram of experimental procedures used in this study.

10% FBS and penicillin-streptomycin) for confocal microscopy imaging. For all the cell studies, the concentration (based on the dye) used for CLLNPs was 0.1 μM , 5 μM and 10 μM for DiI-LDL, LDL-FITC and (Fluo-BOA)LDL, respectively. To evaluate the cellular pathway, A549 cells were co-incubated with CLLNPs and 0.5 μL Alexa Fluor 633 conjugated transferrin (F23362, Molecular Probes) for 4 h and 8 h. After washing with PBS twice, confocal imaging was performed on an Olympus FV1000 laser confocal scanning microscopy (Olympus, Tokyo, Japan) with the excitation wavelength of 488 nm (exciting FITC and Fluo-BOA) or 543 nm (exciting DiI), and 633 nm (exciting Alexa Fluor-transferrin). The binding competition study was conducted by incubation with CLLNPs in the presence of 20-fold excess free LDL in A549 cells. For the PCI study, A549 cells were co-incubated with CLLNPs and 10 $\mu\text{g mL}^{-1}$ AIPcS2a for 8 h. The cells were washed with PBS prior to confocal imaging. To initiate PCI, cells were irradiated with 633 nm laser (40% laser power) for 15 s. Fluorescence imaging was performed with dual channel, 488 nm or 543 nm for CLLNPs and 633 nm (5% of laser power) channel for AIPcS2a. Images were taken before, immediately after, 2 min and 5 min post laser irradiation. Confocal micrographs were analyzed using the Image-J software package. Average cell fluorescence was determined by manual contouring cell borders for analysis. The amount of dye released in the cell cytosol following light stimulation was taken as the difference in average cell fluorescence before and after light exposure.

Results and discussion

Preparation and characterization of CLLNPs

To mimic the ways therapeutic cargo can be loaded in LDL nanoparticles, three types of dyes were introduced *via* the approaches depicted in Fig. 1: (1) Hydrophilic fluorescein (FITC) was loaded onto LDL by conjugation to lysine residues of apoB *via* a thiourea bond (protein-labeling). (2) Hydrophobic Fluo-BOA dye, which consists of two oleoyl groups conjugated to fluorescein, was core-loaded into LDL by a reconstitution method. (3) The fluorescent dye 1,1'-dioctadecyl-3,3',3'-tetramethylindocarbocyanine (DiI) was intercalated into the nanoparticles by surface loading. The number of dyes contained in each LDL nanoparticle was calculated by dividing the concentration of the loaded dye by the LDL concentration. Their morphology and integrity, surface properties, absorption and size were evaluated by electron microscope, gel electrophoresis, spectrophotometry and dynamic light scattering (DLS) respectively. The resulting LDL-FITC, (Fluo-BOA)LDL and DiI-LDL nanoparticles had fluorescent dye payloads of 37, 250 and 30, respectively. As shown in Fig. 3A, all the CLLNPs displayed a high level of monodispersity and spherical size distribution that was similar to native LDL nanoparticles by TEM images, indicating the integrity of the CLLNPs remained intact for the various preparations. The DiI-LDL and (Fluo-

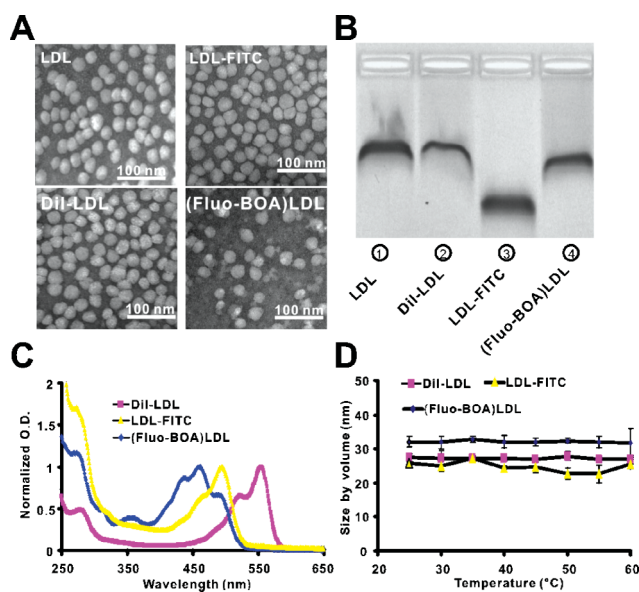


Fig. 3 Characterization of CLLNPs. (a) Transmission electron micrographs of CLLNPs stained with 0.5% uranyl acetate. (b) Gel electrophoresis of CLLNPs using a 0.8% agarose gel stained with coomassie blue. (c) Measurement of the absorption of CLLNPs. (d) Thermostability of CLLNPs at temperatures from 25–60 °C measured by dynamic light scattering (DLS).

BOA)LDL nanoparticles maintained the same gel electrophoresis patterns as LDL nanoparticles (Fig. 3B). FITC-LDL showed faster gel electrophoresis mobility because of the negative charges of FITC combined with the loss of free lysine amines during conjugation, indicating that fluorescein effectively labeled those LDL nanoparticles. The maximum absorption peaks of FITC-LDL, DiI-LDL and (Fluo-BOA)LDL were 490 nm, 554 nm and 458 nm, respectively (Fig. 3C), which were distinguishable from the photosensitizer AIPcS2a (670 nm) used in the PCI treatment (data not shown). Moreover, when varying the temperature from 25–60 °C, all the CLLNPs showed negligible changes in size, demonstrating their thermal stability.

Cellular uptake of CLLNPs

To validate that CLLNPs retained similar biofunctional behavior as native LDL nanoparticles, cell uptake studies were performed in human non-small cell lung cancer A549 cells. Transferrin labeled with Alexa Fluor 633 was used as an early endosome marker. As the confocal microscope images shown in Fig. 4, the intracellular localization of these three different CLLNPs was highly colocalized with transferrin both at early 4 h and late 8 h incubation time points, suggesting their intracellular pathway was similar to transferrin. This was further evidenced by the observation of their punctuate cellular distribution in cells (Fig. 5; red dots for DiI and green dots for FITC and Fluo-BOA), indicating CLLNPs were within endo/lysosome compartment after 8 h incubation. Furthermore, cellular uptake of these CLLNPs was significantly inhibited by adding a 20-fold excess of LDL, suggesting the uptake of CLLNPs was mediated by the LDL receptor. Together, all these data suggest cellular uptake of CLLNPs was through LDL receptor mediated endocytosis.

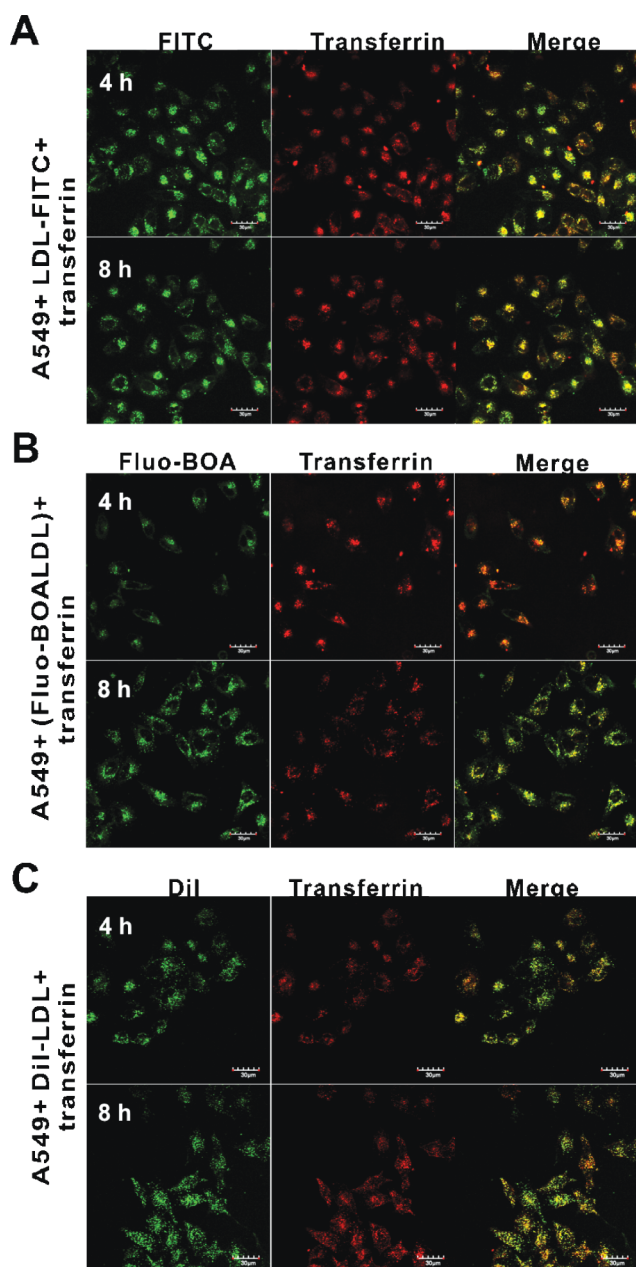


Fig. 4 Examination of the intracellular uptake pathway of CLLNPs. A549 cells were incubated with transferrin as an early endosome maker at 4 h and 8 h incubation along with. (a) LDL-FITC. (b) (Fluo-BOA)LDL. (c) LDL-DiI prior to imaging using confocal microscopy.

PCI of CLLNPs

After verifying the intracellular uptake pathway of CLLNPs, we next tested the use of PCI for cytosolic payload delivery. Following 8 h incubation with CLLNPs and AIPcS2a, confocal imaging of the A549 cells was performed using two channels, one for the LDL loaded dye (FITC and Fluo-BOA, 488 nm; DiI, 543 nm laser), the other channel for tracking the AIPcS2a PCI agent (633 nm laser, 5% of laser power). Cells were then exposed to higher power 633 nm confocal laser light (40% of laser power) for 15 s with a measured power of 1.8 mW, and images then were acquired immediately, 2 and 5 min post irradiation with the previous described dual channel. As shown in Fig. 6A, both DiI-LDL and

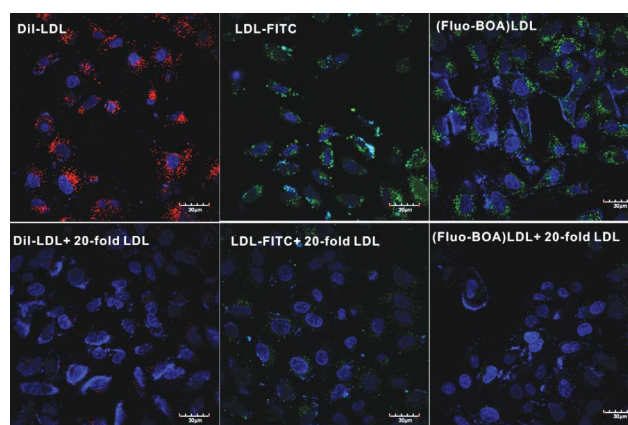


Fig. 5 LDL receptor mediated cellular delivery of CLLNPs. Uptake of CLLNPs in A549 cells with or without the presence of 20-fold excess of LDL nanoparticles competition imaged with confocal microscopy after 8 h incubation. Nuclei are shown in blue.

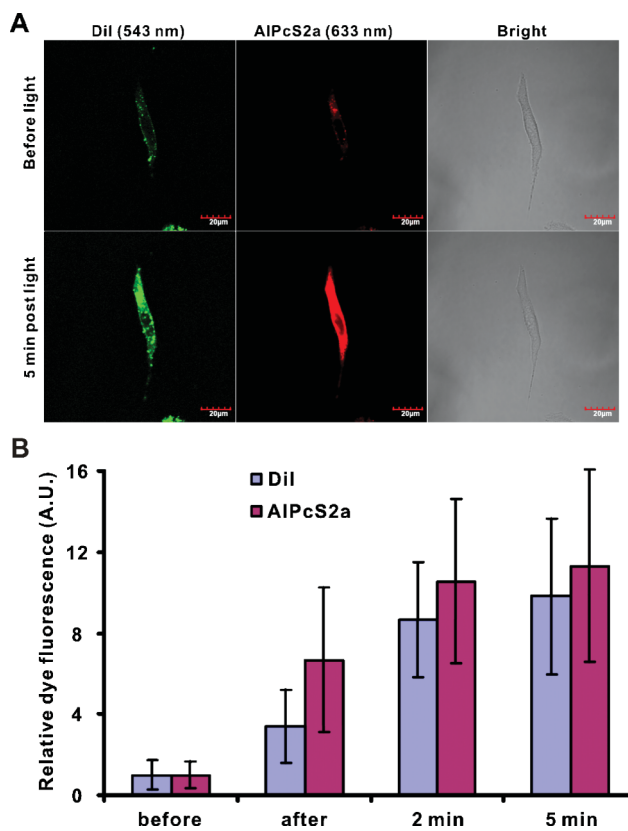


Fig. 6 Evaluation of PCI induced cytosolic release of surface-loaded cargo. (a) Cellular localization of DiI-LDL in A549 cells before and 5 min post light irradiation using live cell confocal microscopy. The green and red signals represented DiI dye and photosensitizer AIPcS2a, respectively. (b) Measurement of the average fluorescence intensity changes before, immediate after, 2 min and 5 min after light irradiation (normalized to initial fluorescence). Data was acquired from 18 cells from at least 3 fields of view.

AIPcS2a were internalized into endolysosomes of A549 cells at 8 h incubation (shown as green and red, respectively). When treated with the 633 nm laser for 15 s, the DiI dye rapidly transferred from the endolysome membranes to the cytosol, similarly to the

AlPcS2a PCI agents. A large amount of DiI and AlPcS2a signals appeared in the confocal images 5 min post laser irradiation. Not only did the cellular distribution change dramatically, but the overall fluorescence intensity increased, likely as a result of reversal of fluorescence quenching induced by low pH or self-aggregation encountered in the endosomes and lysosomes. As shown in Fig. 6B, there was a 3.4-fold increase in DiI signal immediately following light treatment, an 8.7-fold increase after 2 min and 9.8-fold at 5 min. Quantitatively, the signal increase was similar to that of AlPcS2a, which indicated the surface-loaded DiI dye could be efficiently released from endolysosomes to the cytoplasm using PCI.

Next, we evaluated the core-loaded cargo release using PCI. As shown in Fig. 7A, as with the surface loaded CLLNPs, the AlPcS2a dyes relocated into the cytosol and distributed evenly inside the cells (beside nucleus) 5 min post light irradiation, indicating effective disruption of endolysosomal membranes. However, changes in Fluo-BOA distribution or intensity were not observed compared the distribution prior to light treatment. Image analysis demonstrated major increases in the ALPcS2a fluorescent signal, but no significant changes were observed for the Fluo-BOA post laser irradiation (Fig. 7B). These data suggest that the core-loaded cargo Fluo-BOA was not able to release into cytoplasm by PCI.

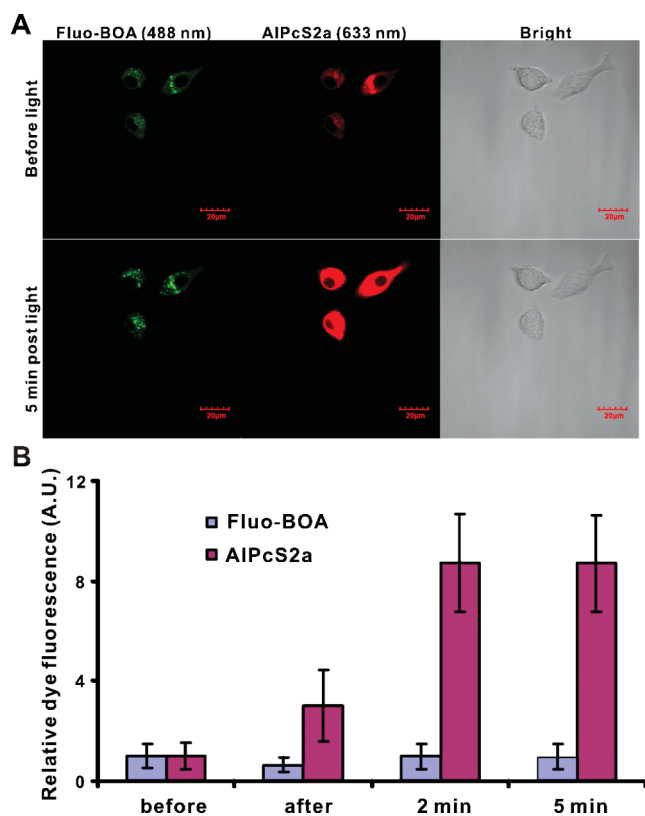


Fig. 7 Evaluation of PCI induced cytosolic release of core-loaded cargo. (a) Confocal real-time imaging the cellular localization of (Fluo-BOA)LDL in A549 cells before and 5 min after light irradiation. The green and red signals represent Fluo-BOA dye and photosensitizer AlPcS2a, respectively. (b) Measurement of the average fluorescence intensity changes before, immediate after, 2 min and 5 min post light irradiation (normalized to initial fluorescence). Data was acquired from 18 cells from at least 3 fields of view.

Finally, we tested whether PCI could facilitate the release of the protein conjugated cargo. As expected, the AlPcS2a PCI-inducing dye could effectively release from endolysosomal organelles to the cytosol in A549 cells within 5 min (Fig. 8A). At the same time, the FITC signal (the green channel in Fig. 8B) spread to the cytoplasm of the cells, resulting in a 2.2 and 2.4-fold signal increase, immediately after and at 5 min post light irradiation, respectively. This release was less efficacious than the photosensitizer AlPcS2a which showed an 8.3-fold signal increase at 5 min post light irradiation, suggesting a partial cargo release from the protein-loaded cargo.

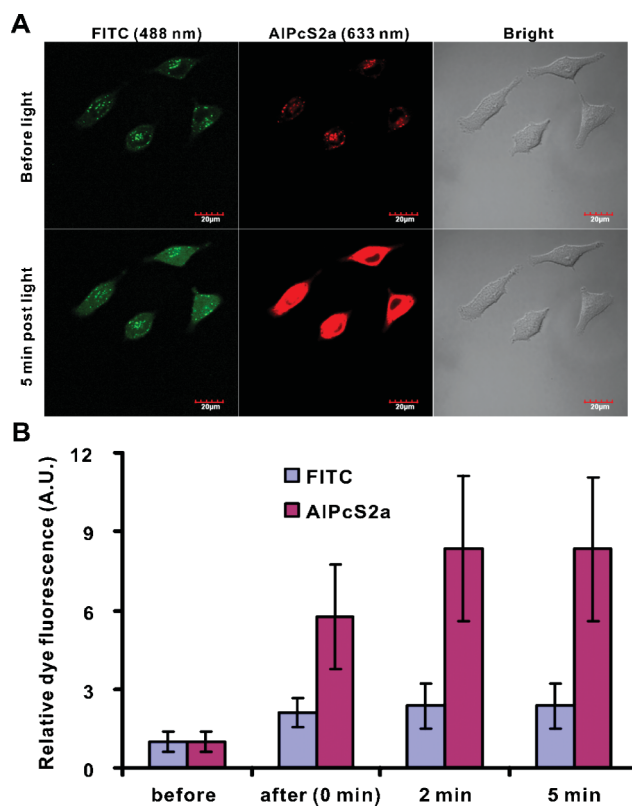


Fig. 8 Evaluation of PCI induced cytosolic release of protein-loaded cargo. (a) Confocal real-time imaging the cellular localization of LDL-FITC in A549 cells before and 5 min after light irradiation. The green and red signals represented FITC dye and photosensitizer AlPcS2a, respectively. (b) Measurement of the average fluorescence intensity changes before, immediate after, 2 min and 5 min post light irradiation (normalized to initial fluorescence). Data was acquired from 18 cells from at least 3 fields of view.

The LDL receptor is over expressed in numerous cancer cells and functions in coordinating the metabolism of cholesterol, an essential component of plasma membrane of all mammalian cells.⁹ The receptor is recycled to the cell surface every 10 min for a total of several hundred trips in its 20 h lifespan, which enables it to carry a large amount of LDL nanoparticles into the cells.¹⁰ LDL nanoparticles are destined to the lysosome after endocytosis inside cells with concomitant degradation of the cargo within a few hours, resulting in destruction of apoB and their phospholipids framework by hydrolysis.⁸ Here we showed that PCI was an effective method for cytosolic release of LDL surface-loaded DiI dye. In contrast, only partial release of

protein-conjugated FITC cargo could be achieved and the core-loaded dye Fluo-BOA could not efficiently release from endolysosomes. These differentiated release mechanisms were presumably due to the various cargo loading methods. (1) The surface loaded dye DiI, with two alkyl chains that can insert into the LDL phospholipid monolayer, as it is commonly used for labeling membranes and lipoproteins.²⁷ After co-endocytosis with LDL particles into cells, DiI dye may transfer from LDL to the endolysosomal membranes or maintain interactions with phospholipids debris. Thus, when the endolysosomal membranes were destroyed by PCI, the increase in fluorescent intensity was detected due to unquenching of DiI after its release into the cytoplasm. (2) In the case of the Fluo-BOA cargo, it was incorporated into the LDL particles by organic solvent evaporation method resulting in entrapment of Fluo-BOA in the core of the nanoparticle in a hydrophobic cluster. When treated by PCI, this hydrophobic cluster did not release and redisperse into the cytoplasm. This phenomenon was also observed in a recent report.²⁸ The hydrophobicity of the cargo was likely a factor in preventing the cytosolic redistribution. (3) Because of the hydrolysis of apoB in the endolysosomes, the FITC-conjugated apoB in CLLNPs might be degraded into larger or smaller polypeptides. The large portions may not be released instantly, while the small amino acid debris could be released using PCI. Thus, only partial release of protein-loaded cargo FITC could be achieved.

Native lipoproteins and their derived, synthetic lipoprotein nanoparticles, which mimic the structure and function of the native lipoproteins, have been used as versatile drug loading nanocarriers for new cancer drugs.^{6,29} However, to exert the best use of CLLNPs for significant biological effect may require not only the efficient delivery, but also subsequent release of their cargo into cytoplasm after intracellular endocytosis. Although the PCI method investigated here could not accelerate the cytosolic release of the LDL core-loaded hydrophobic cargo during a short period of time, the surface-loaded and protein-loaded cargo could be successfully released into cytoplasm.

PCI has broad potential for CLLNPs. For instance, it has been reported that preloading cholesterol modified siRNA (cholesterol-siRNA) into lipoproteins facilitated their biodistribution and enhanced *in vivo* gene silencing efficacy.³⁰ However, a high dose of siRNAs (10–50 mg kg⁻¹) was required to achieve the therapeutic effect mainly because of the inefficient release of siRNAs into cytosol. Theoretically, PCI has potential to benefit such applications and dramatically improve their therapeutic index. Photosensitizer-induced cytotoxicity is an inherent issue with PCI and further study is warranted to find the optimal range of light doses where PCI of LDL nanoparticle cargos is achieved but cell viability is minimally affected.

Conclusions

In summary, this study demonstrated that the cytosolic release of LDL cargo using PCI was feasible and the efficiency was dependent on the cargo loading method. The direct endolysosomal disruption by PCI resulted in rapid intracellular cytosolic release of surface-loaded and partial release of protein-loaded cargo. This provides a promising strategy to bypass the challenges of endolysosomal entrapment, making lipoprotein nanoparticles a more efficacious platform for drug delivery.

Acknowledgements

This study was conducted with the support of the Ontario Institutes for Cancer Research, the Canadian Institute of Health Research, the Natural Sciences and Engineering Research Council of Canada, the China-Canada Joint Health Research Initiative (CIHR CCI-102936, NSFC-30911120489), and the Joey and Toby Tanenbaum/Brazilian Ball Chair in Prostate Cancer Research.

References

- 1 R. A. Firestone, Low-density lipoprotein as a vehicle for targeting antitumor compounds to cancer cells, *Bioconjugate Chem.*, 1994, **5**, 105–113.
- 2 B. Lundberg, Preparation of drug-low density lipoprotein complexes for delivery of antitumor drugs via the low density lipoprotein pathway, *Cancer Res.*, 1987, **47**, 4105–4108.
- 3 S. Vitols, K. Soderberg-Reid, M. Masquelier, B. Sjoström and C. Peterson, Low density lipoprotein for delivery of a water-insoluble alkylating agent to malignant cells. In vitro and in vivo studies of a drug-lipoprotein complex, *Br. J. Cancer*, 1990, **62**, 724–729.
- 4 G. Zheng, J. Chen, H. Li and J. D. Glickson, Rerouting lipoprotein nanoparticles to selected alternate receptors for the targeted delivery of cancer diagnostic and therapeutic agents, *Proc. Natl. Acad. Sci. U. S. A.*, 2005, **102**, 17757–17762.
- 5 J. Chen, I. R. Corbin, H. Li, W. Cao, J. D. Glickson and G. Zheng, Ligand conjugated low-density lipoprotein nanoparticles for enhanced optical cancer imaging *in vivo*, *J. Am. Chem. Soc.*, 2007, **129**, 5798–5799.
- 6 I. R. Corbin and G. Zheng, Mimicking nature's nanocarrier: synthetic low-density lipoprotein-like nanoparticles for cancer-drug delivery, *Nanomedicine*, 2007, **2**, 375–380.
- 7 J. F. Lovell, H. Jin, K. K. Ng and G. Zheng, Programmed nanoparticle aggregation using molecular beacons, *Angew. Chem., Int. Ed.*, 2010, **49**, 7917–7919.
- 8 M. S. Brown and J. L. Goldstein, Receptor-mediated endocytosis: insights from the lipoprotein receptor system, *Proc. Natl. Acad. Sci. U. S. A.*, 1979, **76**, 3330–3337.
- 9 S. Vitols, Uptake of low-density lipoprotein by malignant cells—possible therapeutic applications, *Cancer Cells*, 1991, **3**, 488–495.
- 10 J. L. Goldstein and M. S. Brown, The LDL receptor and the regulation of cellular cholesterol metabolism, *J. Cell Sci. Suppl.*, 1985, **3**, 131–137.
- 11 N. Andre, D. Braguer, G. Brasseur, A. Goncalves, D. Lemesle-Meunier, S. Guise, M. A. Jordan and C. Briand, Paclitaxel induces release of cytochrome c from mitochondria isolated from human neuroblastoma cells, *Cancer Res.*, 2000, **60**, 5349–5353.
- 12 B. Lebleu, Delivering information-rich drugs—prospects and challenges, *Trends Biotechnol.*, 1996, **14**, 109–110.
- 13 K. Berg, P. K. Selbo, L. Prasmickaite, T. E. Tjelle, K. Sandvig, J. Moan, G. Gaudernack, O. Fodstad, S. Kjolsrud, H. Anholt, G. H. Rodal, S. K. Rodal and A. Hogset, Photochemical internalization: a novel technology for delivery of macromolecules into cytosol, *Cancer Res.*, 1999, **59**, 1180–1183.
- 14 A. Dietze, P. K. Selbo, L. Prasmickaite, A. Weyergang, A. Bonsted, B. Engesaeter, A. Hogset and K. Berg, Photochemical internalization (PCI): a new modality for light activation of endocytosed therapeutics, *J. Environ. Pathol. Toxicol. Oncol.*, 2006, **25**, 521–536.
- 15 K. Berg, M. Folini, L. Prasmickaite, P. K. Selbo, A. Bonsted, B. O. Engesaeter, N. Zaffaroni, A. Weyergang, A. Dietze, G. M. Maeldansmo, E. Wagner, O. J. Norum and A. Hogset, Photochemical internalization: a new tool for drug delivery, *Curr. Pharm. Biotechnol.*, 2007, **8**, 362–372.
- 16 A. Dietze, A. Bonsted, A. Hogset and K. Berg, Photochemical internalization enhances the cytotoxic effect of the protein toxin gelonin and transgene expression in sarcoma cells, *Photochem. Photobiol.*, 2003, **78**, 283–289.
- 17 A. Dietze, B. Engesaeter and K. Berg, Transgene delivery and gelonin cytotoxicity enhanced by photochemical internalization in fibroblast-like synoviocytes (FLS) from rheumatoid arthritis patients, *Photochem. Photobiol. Sci.*, 2005, **4**, 341–347.
- 18 M. Folini, K. Berg, E. Mollo, R. Villa, L. Prasmickaite, M. G. Daidone, U. Benatti and N. Zaffaroni, Photochemical internalization of a peptide nucleic acid targeting the catalytic subunit of human telomerase, *Cancer Res.*, 2003, **63**, 3490–3494.

- 19 O. J. Norum, J. V. Gaustad, E. Angell-Petersen, E. K. Rofstad, Q. Peng, K. E. Giercksky and K. Berg, Photochemical internalization of bleomycin is superior to photodynamic therapy due to the therapeutic effect in the tumor periphery, *Photochem. Photobiol.*, 2009, **85**, 740–749.
- 20 S. Oliveira, A. Hogset, G. Storm and R. M. Schiffelers, Delivery of siRNA to the target cell cytoplasm: photochemical internalization facilitates endosomal escape and improves silencing efficiency, in vitro and in vivo, *Curr. Pharm. Des.*, 2008, **14**, 3686–3697.
- 21 P. K. Selbo, A. Weyergang, A. Høgset, O. J. Norum, M. B. Berstad, M. Vikdal and K. Berg, Photochemical internalization provides time- and space-controlled endolysosomal escape of therapeutic molecules, *J. Controlled Release.*, 2010, **148**, 2–12.
- 22 P. S. Lai, P. J. Lou, C. L. Peng, C. L. Pai, W. N. Yen, M. Y. Huang, T. H. Young and M. J. Shieh, Doxorubicin delivery by polyamidoamine dendrimer conjugation and photochemical internalization for cancer therapy, *J. Controlled Release*, 2007, **122**, 39–46.
- 23 M. M. Fretz, A. Hogset, G. A. Koning, W. Jiskoot and G. Storm, Cytosolic delivery of liposomally targeted proteins induced by photochemical internalization, *Pharm. Res.*, 2007, **24**, 2040–2047.
- 24 K. Raemdonck, B. Naeye, A. Hogset, J. Demeester and S. C. De Smedt, Prolonged gene silencing by combining siRNA nanogels and photochemical internalization, *J. Controlled Release*, 2010, **145**, 281–288.
- 25 R. J. Havel, H. A. Eder and J. H. Bragdon, The distribution and chemical composition of ultracentrifugally separated lipoproteins in human serum, *J. Clin. Invest.*, 1955, **34**, 1345–1353.
- 26 M. Krieger, L. C. Smith, R. G. Anderson, J. L. Goldstein, Y. J. Kao, H. J. Pownall, A. M. Gotto Jr. and M. S. Brown, Reconstituted low density lipoprotein: a vehicle for the delivery of hydrophobic fluorescent probes to cells, *J. Supramol. Struct.*, 1979, **10**, 467.
- 27 H. Li, Z. Zhang, D. Blessington, D. S. Nelson, R. Zhou, S. Lund-Katz, B. Chance, J. D. Glickson and G. Zheng, Carbocyanine labeled LDL for optical imaging of tumors, *Acad. Radiol.*, 2004, **11**, 669–677.
- 28 S. Febvay, D. M. Marini, A. M. Belcher and D. E. Clapham, Targeted cytosolic delivery of cell-impermeable compounds by nanoparticle-mediated, light-triggered endosome disruption, *Nano Lett.*, 2010, **10**, 2211–2219.
- 29 M. Nikanjam, E. A. Blakely, K. A. Bjornstad, X. Shu, T. F. Budinger and T. M. Forte, Synthetic nano-low density lipoprotein as targeted drug delivery vehicle for glioblastoma multiforme, *Int. J. Pharm.*, 2007, **328**, 86–94.
- 30 C. Wolfrum, S. Shi, K. N. Jayaprakash, M. Jayaraman, G. Wang, R. K. Pandey, K. G. Rajeev, T. Nakayama, K. Charrise, E. M. Ndungo, T. Zimmermann, V. Kotliansky, M. Manoharan and M. Stoffel, Mechanisms and optimization of in vivo delivery of lipophilic siRNAs, *Nat. Biotechnol.*, 2007, **25**, 1149–1157.